

Original Research

# Degradation of Chloramphenicol by VUV/Peroxymonosulfate Process: Kinetics, Effects of Water Matrix Components, Modeling and Economic Optimization

Xing Zhang<sup>1,2</sup>, Jinghan Liu<sup>1,2\*</sup>, Yizi Liu<sup>1,2</sup>, Changhua Lu<sup>1\*\*</sup>, Shuqing Li<sup>1,2</sup>, Zhen Zhou<sup>3</sup>

<sup>1</sup>Naval Logistics Academy, Tianjin 300000, China

<sup>2</sup>Unit 91292 of PLA, Baoding, 074000, China

<sup>3</sup>State Key Laboratory of Technologies in Space Cryogenic Propellants, Beijing Special Engineering Design and Research Institute, Beijing 100028, China

Received: 8 August 2024

Accepted: 2 December 2024

## Abstract

As a cost-effective and wide-spectrum antibiotic with potent antibacterial properties, CAP (chloramphenicol) has been widely used in aquaculture and human medicine in recent years and is difficult to degrade by traditional biological treatment methods. In this study, the kinetics and economy in the oxidization of CAP by the VUV/PMS (peroxymonosulfate) process were investigated. The degradation of CAP was exhibited remarkably by the VUV/PMS process, compared with the individual effects of VUV and PMS. The degradation reaction followed pseudo-zero-order kinetics, with  $R^2$  of 0.993, indicating a relatively constant rate of degradation under certain conditions. Quenching experiments revealed that hydroxyl radicals ( $\bullet\text{OH}$ ) played a predominant role in the reaction. The degradation process was simulated effectively by a quadratic polynomial model, with degradation efficiency as the response variable and dosages of PMS, UV power, and retention time as independent variables, utilizing response surface methodology (RSM). The lowest total operating cost for CAP degradation was determined to be 0.417 USD/m<sup>3</sup>/order.

**Keywords:** VUV/peroxymonosulfate, chloramphenicol, hydroxyl radicals, response surface methodology

## Introduction

As one of the most pivotal medical advancements in human history, antibiotics have saved countless lives with

their application in the medical industry. Nevertheless, the abuse of antibiotics in the medical field has sparked widespread concern in recent years [1]. A significant challenge arises from the fact that most antibiotics are not fully metabolized by humans, leading to antibiotics being released into the natural environment via feces and urine [2]. Moreover, the extensive use of antibiotics in the livestock industry, particularly the administration

\*e-mail: 1226001717@qq.com

Tel.: +86-17638585221

\*\*e-mail: 18032878089@163.com

Tel.: +86-18032878089

of antibiotics in animal feed as a prophylactic measure against bacterial infections, further exacerbates the risk of antibiotic contamination in the environment [3].

Chloramphenicol (CAP), a prototypical antibiotic, has been widely employed in recent years due to its cost-effectiveness and broad-spectrum antibacterial activity [4]. Potential sources of CAP contamination in aquatic environments encompass pharmaceutical manufacturers, sewage treatment plants, and hospital wastewater treatment facilities [5]. Kimosop et al. [6] observed concentrations of CAP ranging from 60 to 100 ng/L in some hospital wastewater. Furthermore, CAP concentrations as high as 100-500 ng/L have been detected in some wastewater treatment systems [7-9]. It has been documented that the presence of CAP in natural surface waters, with concentrations of 1-15 ng/L identified in Singapore's surface water sources [10] and 15.52-24.35 ng/L in Malaysian rivers [11]. Relevant literature has also been reported in China, where CAP as high as 11-266 ng/L was found in the Pearl River [12], and 4.2-28.4 ng/L CAP was found in the Huangpu River in Shanghai [13]. Notably, many of these rivers serve as drinking water sources, posing a significant concern. Unwitting ingestion of antibiotics, even under healthy conditions, will promote bacterial resistance, exacerbating the challenge of finding effective treatments against bacterial infections. Moreover, studies have shown that CAP, which readily bioaccumulates through the food chain into humans, exhibits bone marrow toxicity and may lead to aplastic anemia [14, 15]. Owing to the antibacterial nature of CAP, traditional biological treatment processes struggle to achieve satisfactory results. Consequently, oxidation-based processes have garnered increasing attention [16, 17].

Advanced oxidation processes (AOPs), renowned for their exceptional oxidative capabilities, have been noticed as a research frontier in recent years for the degradation of recalcitrant organic compounds such as personal care products and antibiotics [18, 19]. Within this category, various means, including heat, transition metals, photocatalysts, ultrasonics, and ultraviolet (UV) radiation, are employed to activate oxidants, generating free radicals that subsequently oxidize organic pollutants [20]. However, thermal activation, due to the large specific heat capacity of water, necessitates substantial energy consumption to elevate water temperatures, thereby limiting its applicability. While transition metal-mediated activation demonstrates effectiveness, its high cost and the toxicity of most transition metal ions pose challenges for large-scale implementation in water treatment processes. Nanocatalysts, though promising, face difficulties in practical applications due to difficulties in recovery and susceptibility to poisoning after repeated use. Among these, clean and green activation methods have garnered significant attention, particularly in settings with limited technological resources, such as remote islands, where ecological sensitivity is high and constraints exist in terms of

sewage treatment equipment, chemicals, and recovery conditions.

In recent years, UV-based advanced oxidation (UV-AOPs) processes have emerged as a research focus and highlight the degradation of CAP due to their green, environmentally friendly, and non-secondary pollution characteristics. Despite the promising overall degradation efficiency achieved by previously reported UV-AOPs, these methods often suffer from prolonged retention time. For instance, Rizzo et al. [21] achieved near-complete degradation of CAP within 2 hours using the UV/hydrogen peroxide (UV/H<sub>2</sub>O<sub>2</sub>) process. Similarly, Tan et al. [22] reported a degradation efficiency exceeding 90% with the UV/persulfate (UV/PS) process, but this was also accompanied by a long retention time of approximately 2 hours, resulting in the electrical energy per order (EE/O) of 16.76 kWh/m<sup>3</sup>/order.

As the current economic inefficiency of UV-based processes, this study aims to explore more efficient and cost-effective alternative technologies. Previous experiments and literature reviews have revealed that the UV/PMS (peroxymonosulfate) process exhibits promising performance in degrading various organic pollutants, particularly in the treatment of oxytetracycline, another antibiotic, where it outperformed UV/H<sub>2</sub>O<sub>2</sub> significantly [23]. However, to our knowledge, there is a lack of reported assessments on the degradation efficiency of CAP with PMS activated by UV, let alone VUV. Compared to UV lamps, VUV lamps could emit light at 185 nm, featuring a shorter wavelength and higher photon energy, which holds the promise of further reducing the retention time required for the oxidation process and, consequently, lowering the overall energy consumption, rendering it more economically viable for industrial applications. Additionally, VUV retains the environmentally friendly advantages of UV. Therefore, the combination of VUV with PMS represents a highly promising process for the oxidative degradation of antibiotics, potentially enabling stable operation at a lower cost while achieving green and efficient degradation of pollutants. Consequently, this study endeavors to investigate the degradation efficiency of CAP by the VUV/PMS process and optimize the process parameters utilizing RSM, thereby offering an environmentally friendly and cost-effective CAP treatment approach that combines high efficiency with low costs.

## Materials and Methods

### Chemical

Peroxymonosulfate (KHSO<sub>5</sub>·0.5KHSO<sub>4</sub>·0.5K<sub>2</sub>SO<sub>4</sub>, AR grade) was procured from Aladdin (Shanghai, China). Chloramphenicol was purchased from Biosharp Life Sciences Co., Ltd. (Beijing, China). Ethanol (AR grade) was sourced from Xilong Scientific Co., Ltd.

(Guangdong, China). The sulfuric acid standard solution (0.5 M) was acquired from Codow Pharma Tech Co., Ltd. (Guangdong, China). Isopropyl alcohol (AR grade) was purchased from Hengxing Chemical Preparation Co., Ltd. (Tianjin, China). Sodium nitrate standard solution (0.5 M) was obtained from Kermel Chemical Reagents Co., Ltd. (Tianjin, China). Sodium hydroxide (AR grade), sodium chloride (AR grade), and sodium sulfate (AR grade) were purchased from National Chemical Reagent Co. (Chongqing, China). Disodium hydrogen phosphate (AR grade), sodium dihydrogen phosphate (AR grade), and sodium bicarbonate (AR grade) were sourced from Tianjin Damao Chemical Reagent Factory (Tianjin, China). Solutions were prepared with double deionized water (18.2 MΩ cm).

### Analysis

The concentration of CAP was measured utilizing the spectrophotometric method. At predetermined time intervals, samples were withdrawn from the reaction mixture and injected into a 1 cm quartz cuvette equipped with an ultraviolet-visible spectrophotometer (Hach DR6000, USA). The absorbance of the samples at 278 nm was then recorded to quantify the CAP concentration [24]. The pH of the solutions was measured using a pH meter (Hanna, HI98107, Italy).

### Experimental Procedures

The photodegradation was conducted within a cylindrical glass reactor with a diameter of 10 cm and a height of 30 cm, placed in a constant temperature water bath maintained at 25°C. A magnetic stirring bar rotating at 400 rpm was positioned at the bottom of the reactor to ensure uniform mixing of the reaction mixture. An ultraviolet lamp (GPH287T5VH/4, 14 W, Heraeus, Germany) encased in a quartz sleeve was vertically inserted into the cylindrical reactor to ensure even distribution of radiation throughout the reaction system. The low-pressure mercury lamp used in the experiment primarily emitted UV light at wavelengths of 185 nm and 254 nm. A specific dosage of PMS was added to 2 L of the reaction mixture, with an initial CAP concentration of 6 μM. Phosphate buffer solution (6 mM) was employed to adjust the pH of the reaction system, as phosphates exhibit negligible interference with radical-mediated oxidation processes

[25]. The specific pH adjustment procedure involved slowly adding sulfuric acid or sodium hydroxide to a phosphate buffer solution (6 mM) with an initial pH of 7.0 while continuously monitoring and recording the pH of the solution. The addition of sulfuric acid or sodium hydroxide was halted once the desired pH was achieved. Specific lengths of aluminum foil were used to wrap the UV lamp tube and modulate its power output. Following a designated reaction time, 2.5 mL of the reaction mixture was immediately withdrawn for analysis and measurement.

### Response Surface Experiment Design

The degradation process was optimized by RSM, utilizing dosages of PMS, UV power, and reaction time as independent variables, while the degradation efficiency of CAP and the total operating cost of the process serve as the response values for optimization. The Box-Behnken Design (BBD) was adopted for the optimization experiments due to its simplicity and operability. The ranges of the independent variables were determined based on single-factor experiments and previous literature reports, selecting efficient intervals with high degradation efficiency. The specific coded values and ranges are presented in Table 1. A retention time that was too short resulted in insufficient degradation of CAP, failing to achieve the desired degradation effect. Conversely, an excessively long retention time increased electrical consumption while contributing minimally to further enhancements in the degradation efficiency of CAP. According to prior experiments, when the retention time was within the range of 4-14 min, the degradation efficiency of CAP was relatively high. A quadratic polynomial was used to fit and analyze the reactions, facilitated by the Design-Expert 13 software, as shown in Equation (1).

$$Y = \beta_0 + \sum_{i=1}^n \beta_i x_i + \sum_{i=1}^n \beta_{ii} x_i^2 + \sum_{i=1}^{n-1} \sum_{j=1}^n \beta_{ij} x_i x_j + \varepsilon \quad (1)$$

In the Equation, Y represents the response value (degradation efficiency of CAP),  $\beta_0$  denotes the constant term,  $\beta_i$  and  $\beta_{ii}$  represent the linear and quadratic coefficients, respectively, of the independent variable  $X_i$ ,  $\beta_{ij}$  represents the interaction coefficient between  $X_i$  and  $X_j$ , and  $\varepsilon$  stands for the residual term [26].

Table 1. Ranges and levels of the variables for experimental design.

Variables	Code	Unit	Ranges and levels		
			-1	0	1
Dosages of PMS	A	mM	0.2	0.5	0.8
UV power	B	W	3.5	8.75	14
Retention time	C	min	4	9	14

## Results and Discussion

### Photodegradation of CAP by VUV Activated PMS

The results of CAP degradation by VUV alone, PMS alone, and the VUV/PMS process were presented in Fig. 1. As shown in the Fig. 1, the degradation efficiency of CAP under VUV alone was 24%, while that under PMS alone was 7%, and the degradation efficiency achieved by the VUV/PMS process was 99% after 10 min. These observations indicated that the efficiency of the VUV/PMS oxidation process far exceeded that of VUV or PMS acting individually. This superiority stemmed from the stronger oxidizing capacity of the generated radicals compared to PMS. UV radiation could activate and decompose PMS to produce  $\text{SO}_4^{\cdot-}$  (sulfate radicals) and  $\cdot\text{OH}$  (hydroxyl radicals) (Equations (2) and (3)), which possessed redox potentials of 2.5-3.1 V and 1.8-2.7 V, respectively, under neutral conditions. These potentials were higher than that of PMS (1.82 V), enabling the effective degradation of a wide range of pollutants [27-29].

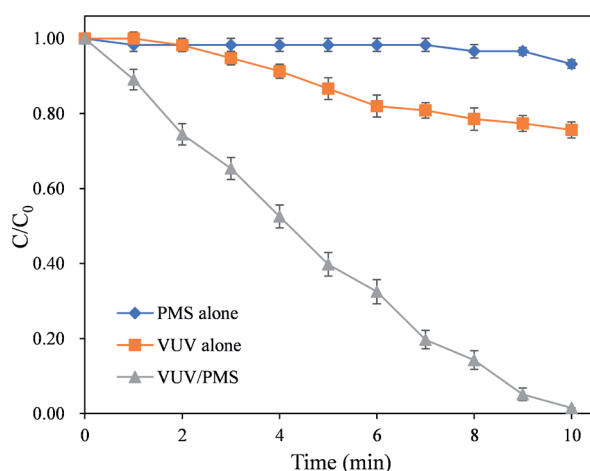
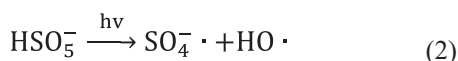
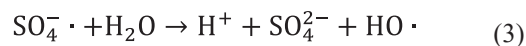


Fig. 1. The degradation of CAP by the VUV alone, PMS alone, and VUV/PMS process. Conditions: initial concentration of CAP = 6  $\mu\text{M}$ , dosages of PMS = 0.4 mM, temperature = 25°C, pH = 7.0, UV power = 14 W.



The fitting results of the degradation kinetic models are presented in Table 2. Among the pseudo-zero-order, pseudo-first-order, and pseudo-second-order kinetic models, the pseudo-zero-order model exhibited the highest  $R^2$  of 0.993, indicating that the reaction follows pseudo-zero-order kinetics. This finding slightly differed from previous studies but aligned with those on thermally activated PS or PMS [30, 31]. Considering that the second-order reaction rate constants between free radicals and organic pollutants were generally high [32], it could be approximated that the lifetime of free radicals in the reaction system was very short, with virtually all generated radicals being instantly consumed by organic compounds. In comparison with other similar UV-activated PMS studies, the present degradation system featured a larger reactor diameter of 10 cm and a higher reaction volume of 2 L, significantly exceeding those in other comparable investigations. Moreover, the intensity of UV irradiation attenuated rapidly with distance, suggesting that the rate-limiting step might be the photon absorption and decomposition of PMS rather than the concentration of CAP. Consequently, the reaction follows pseudo-zero-order kinetics.

As shown in Fig. 2, when the pH was increased to 11 while other conditions remained constant, PMS was activated under alkaline conditions (where the decomposition rate of PMS has been reported to accelerate significantly at pH values greater than 9.4 [23]). Consequently, the decomposition rate accelerated, resulting in the generation of more free radicals. In this case, the decomposition rate of PMS ceased to be the rate-limiting step, and the degradation rate of CAP significantly decreased as the concentration of CAP decreased. The  $R^2$  of the pseudo-second-order kinetics was 0.990 ( $R^2 = 0.756$  for the zero-order model and  $R^2 = 0.961$  for the first-order model), and the reaction followed the pseudo-second-order kinetics. In this case, the reaction rate was related to both the concentration of CAP and the residual concentration of PMS. This phenomenon verifies the above hypothesis that the reaction conformed to the pseudo-zero-order kinetics under neutral conditions.

Table 2. Fitting of different kinetics.

	Zero Order	First Order	Second Order
Rate law	rate = k	rate = k[A]	rate = k[A] <sup>2</sup>
Units for k	mol/(L·s)	1/s	L/(mol·s)
Integrated rate law in straight-line form	$[A]_t = -kt + [A]_0$	$\ln[A]_t = -kt + \ln[A]_0$	$1/[A]_t = kt + 1/[A]_0$
$R^2$	0.993	0.897	0.566

Conditions: initial concentration of CAP = 6  $\mu\text{M}$ , dosages of PMS = 0.4 mM, temperature = 25°C, UV power = 14 W.

### Effect of pH

As depicted in Fig. 2, the reaction rate significantly accelerated with the decrease in pH. At pH 5.0, although the overall degradation efficiency was comparable to that at pH 7.0, the reaction rate notably accelerated, with CAP's concentration decreasing by an order of magnitude within 7 min, resulting in a degradation efficiency of 90%, while under neutral conditions, it was 80%. When pH was adjusted to 3.0, the degradation efficiency approached 90% within approximately 5 min, whereas the degradation efficiency at 5 min was 60% under neutral conditions. This observation aligned with previous research findings, indicating that acidic conditions could enhance the degradation efficiency of the VUV/PMS process. This might be attributed to the fact that under acidic conditions, the redox potential of  $\cdot\text{OH}$  is higher, at 2.7 V, exceeding 1.8 V under neutral conditions, thereby accelerating the reaction rate [33].

With the increase in pH, the reaction rate notably accelerated. When the pH rose from 7 to 9, the degradation efficiency of CAP at 7 min increased from 80% to 89%. At pH 11, despite the overall degradation efficiency being lower than under neutral conditions, it is observable that the initial reaction rate was substantially higher than that under neutral conditions. This phenomenon could be attributed to the accelerated decomposition rate of PMS under alkaline conditions, particularly when  $\text{pH} > 9.4$ . Despite the enhanced reaction rate, the overall degradation efficiency at pH 11 was reduced compared to that at pH 7, which could be explained by the excessively rapid decomposition of PMS leading to a significant increase in the number of radicals within a short period. Consequently, excessive radicals underwent self-quenching reactions (Equations (4) and (5)) and self-combination reactions

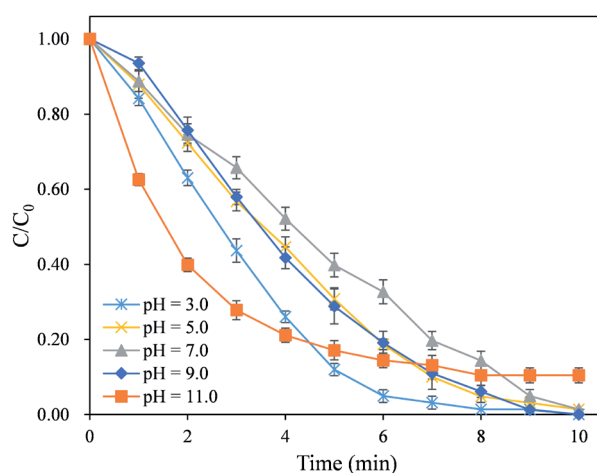
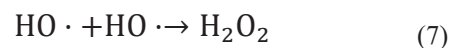
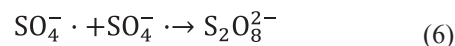
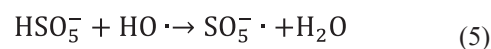
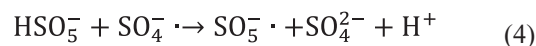


Fig. 2. Effects of pH on the CAP degradation by the VUV/PMS process. Conditions: initial concentration of CAP = 6  $\mu\text{M}$ , dosages of PMS = 0.4 mM, temperature = 25°C, UV power = 14 W.

(Equations (6) and (7)), thereby reducing the overall degradation efficiency [34].



### Effect of PMS Dosage

As shown in Fig. 3, when the dose of PMS was 0.2 mM, 0.4 mM, 0.6 mM, and 0.8 mM, the pseudo-zero kinetic rate of the reaction was  $6.41 \times 10^{-9} \text{ mol}\cdot\text{L}^{-1}\cdot\text{s}^{-1}$ ,  $1.04 \times 10^{-8} \text{ mol}\cdot\text{L}^{-1}\cdot\text{s}^{-1}$ ,  $1.50 \times 10^{-8} \text{ mol}\cdot\text{L}^{-1}\cdot\text{s}^{-1}$ , and  $1.96 \times 10^{-8} \text{ mol}\cdot\text{L}^{-1}\cdot\text{s}^{-1}$ , respectively. According to previous literature, the increase in dosages of PMS could elicit two primary effects: i) Augmented dosages of PMS led to an increase in the number of radicals generated by VUV-activated PMS, thereby enhancing the degradation of CAP [35]; ii) An excessive amount of PMS resulted in an overabundance of radicals, which underwent self-quenching reactions, diminishing the stimulatory effect on CAP degradation and potentially causing adverse effects. In this study, despite the increase in PMS concentration, the threshold level had not been reached, thus exhibiting a pronounced promoting effect as dosages of PMS increased.

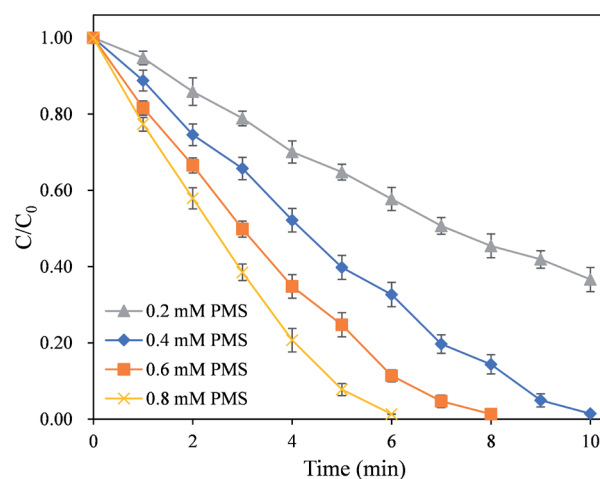


Fig. 3. Effects of dosages of PMS on the CAP degradation by the UV/PMS process. Conditions: initial concentration of CAP = 6  $\mu\text{M}$ , pH = 7.0, temperature = 25°C, UV power = 14 W. The regression equations of 0.2 mM PMS, 0.4 mM PMS, 0.6 mM PMS and 0.8 mM PMS on the CAP degradation by the UV/PMS process were  $y = -0.00641x + 5.82$  ( $R^2 = 0.991$ ),  $y = -0.0104x + 5.67$  ( $R^2 = 0.993$ ),  $y = -0.0150x + 5.92$  ( $R^2 = 0.993$ ) and  $y = -0.0196x + 6.14$  ( $R^2 = 0.994$ ), respectively.

### Effect of UV Power

As depicted in Fig. 4, as the UV power increased from 3.5 W to 14 W, the total degradation efficiency of CAP was observed to be 40%, 67%, 90%, and 99%, with the reaction rate of  $3.89 \times 10^{-9} \text{ mol}\cdot\text{L}^{-1}\cdot\text{s}^{-1}$ ,  $6.70 \times 10^{-9} \text{ mol}\cdot\text{L}^{-1}\cdot\text{s}^{-1}$ ,  $9.06 \times 10^{-9} \text{ mol}\cdot\text{L}^{-1}\cdot\text{s}^{-1}$ ,  $1.04 \times 10^{-8} \text{ mol}\cdot\text{L}^{-1}\cdot\text{s}^{-1}$ , respectively. This phenomenon could be attributed to the enhanced probability of PMS accepting photons as the UV power intensified, thereby accelerating the decomposition rate of PMS and, subsequently, the degradation rate of CAP. Notably, with the increment in UV power, between 3.5 W and 10.5 W, every 3.5 W increase led to a rise in total degradation efficiency of CAP by 27% and 23%, respectively. However, when the UV power was incremented from 10.5 W to 14 W (another 3.5 W increase), the total degradation efficiency of CAP only improved by 9%, significantly less pronounced than the previous increments. It was consistent with previous research on dichloroacetonitrile [36], indicating that the promotional effect of UV power escalation on CAP degradation exhibited a diminishing marginal effect. Once the UV power reached a certain threshold, further increases yield notably diminished benefits to the degradation process, suggesting that blindly enhancing UV power was economically inefficient.

### Effects of Water Matrix Components

Chloride ions, bicarbonate ions, sulfate ions, and nitrate ions are common anions in water and are widely distributed in natural water bodies. In this section, sodium chloride, sodium bicarbonate, sodium sulfate, and sodium nitrate were separately added to the reaction system to investigate the effects of these ubiquitous anions in water on the degradation of CAP by the VUV/PMS process.

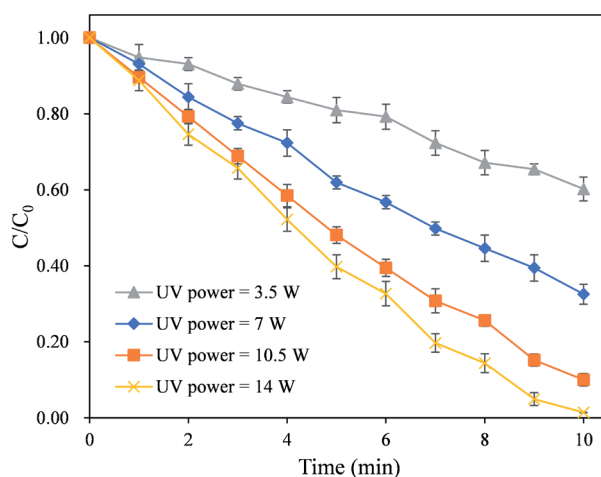
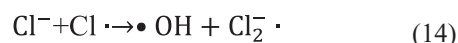
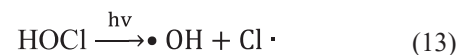
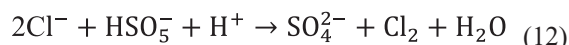
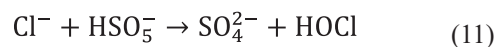
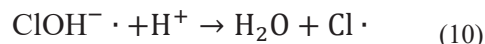
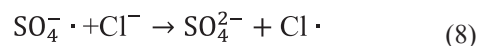
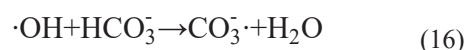
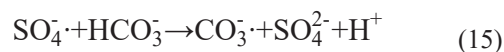


Fig. 4. Effects of UV power on the CAP degradation by the VUV/PMS process. Conditions: initial concentration of CAP = 6  $\mu\text{M}$ , dosages of PMS = 0.4 mM, pH = 7.0, temperature = 25°C.

As shown in Fig. 5, a negligible difference was observed in overall degradation efficiency upon the addition of chloride ions to the reaction system, but the reaction rate slightly accelerated, indicating a weak promotional effect of chloride ions on CAP degradation. According to previous reports, chloride ions exhibit dual opposing effects on such reactions. At low concentrations, chloride ions enhance the reaction by interacting with  $\text{SO}_4^{\cdot-}$  and  $\cdot\text{OH}$  to generate  $\text{Cl}\cdot$  (Equations (8)-(10)), which possesses an oxidation-reduction potential of up to 2.4 V, enabling it to oxidize CAP. Furthermore, chloride ions could react with excess PMS to generate  $\text{Cl}\cdot$  and  $\cdot\text{OH}$  (Equations (11)-(13)), thereby accelerating the reaction. However, in the presence of excessive chloride ions, the formation of  $\text{Cl}_2\cdot$  with a lower oxidation-reduction potential of 1.36 V occurs through the reaction with  $\text{Cl}\cdot$  (Equation (14)), which inhibits the reaction [22, 32]. In the present study, the absence of significant inhibitory effects suggested that the concentration of added chloride ions was relatively low, failing to reach the inhibitory threshold, thus resulting in a slightly promotional effect.



Upon the introduction of bicarbonate ions into the reaction system, a notable decrease in the overall degradation efficiency was observed. As the concentration of bicarbonate ions increased from 0.2 mM to 10 mM, the total degradation efficiency diminished from 99% to 45%. This phenomenon could be attributed to two primary reasons: i) The reaction between  $\text{HCO}_3^-$  and  $\text{SO}_4^{\cdot-}$  or  $\cdot\text{OH}$  resulted in the formation of  $\text{CO}_3^{\cdot-}$ , a significantly weaker oxidant that was ineffective in oxidizing most organic pollutants, as depicted in Equations (15) and (16) [37]; ii) During the quenching process of  $\text{SO}_4^{\cdot-}$  and  $\cdot\text{OH}$  by  $\text{HCO}_3^-$ , certain intermediates were generated, which hindered the formation of radical chain reactions, thereby impeding the progress of the overall reaction [38].



Following the introduction of sulfate ions into the reaction system, minimal changes were observed

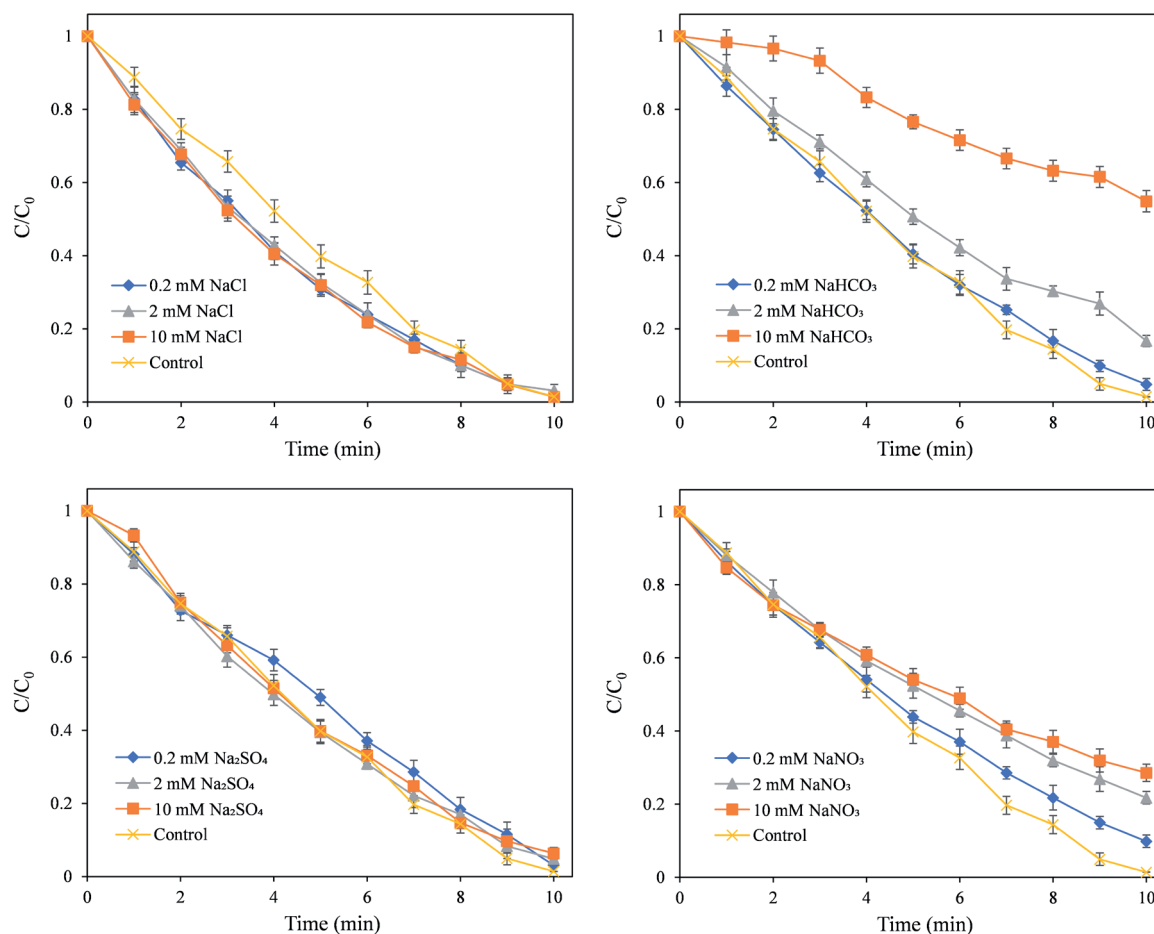
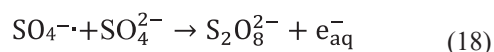
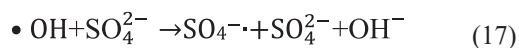


Fig. 5. The influence of water matrix components on the degradation of CAP by the VUV/PMS process. Conditions: initial concentration of CAP = 6  $\mu$ M, dosages of PMS = 0.4 mM, temperature = 25°C, pH = 7.0, UV power = 14 W.

in the overall degradation efficiency, which aligned with previous research. The reactions between sulfate ions and  $\bullet$ OH or  $\text{SO}_4^{\bullet-}$  (Equations (17) and (18)) proceed at a significantly slower rate compared to those with inorganic ions such as chloride and bicarbonate [39]. Consequently, the impact of sulfate ions in the reaction system was negligible.



After incorporating nitrate ions within the reaction environment, a notable decrease in the overall degradation efficiency was evident. As the concentration of nitrate ions increased from 0.2 mM to 10 mM, the total degradation efficiency declined from 99% to 72%. This phenomenon could be attributed to the fact that nitrate ions acted as UV-light shields, absorbing UV radiation and consequently reducing the intensity of UV radiation reaching the PMS molecules. This hindered the photodecomposition of PMS, leading to a decrease in the formation of  $\text{SO}_4^{\bullet-}$  and  $\bullet$ OH. Compelling evidence for this was provided in Fig. S1, showcasing the strong

absorbance of nitrate ions within the vacuum ultraviolet and ultraviolet wavelength range, which overlapped with the primary wavelengths (185 nm and 254 nm) emitted by the UV lamp used in this experiment.

### The Role of Radicals

Quenching experiments were conducted to identify the predominant radical species in the oxidation system. In these quenching experiments, the selection of the quencher was crucial. In the context of alcohols containing  $\alpha$ -hydrogen, the reaction rate constants for the reaction of ethanol with  $\bullet$ OH lie within the range of  $1.2 \times 10^9$  to  $2.8 \times 10^9$   $\text{M}^{-1}\cdot\text{s}^{-1}$ , while those for the reaction with  $\text{SO}_4^{\bullet-}$  fall between  $1.6 \times 10^7$  and  $7.7 \times 10^7$   $\text{M}^{-1}\cdot\text{s}^{-1}$  [40]. These data indicate that both  $\bullet$ OH and  $\text{SO}_4^{\bullet-}$  could react rapidly with ethanol, thereby rendering ethanol a common quencher for these two types of radicals. In systems where both radicals coexist, isopropanol (IPA) effectively quenches  $\bullet$ OH only [23]. Therefore, the dominant radical species could be determined by examining the inhibitory effects of ethanol and IPA on the reaction. As shown in Fig. 6, upon adding 0.5 mM of ethanol and IPA, respectively, to the reaction systems, the

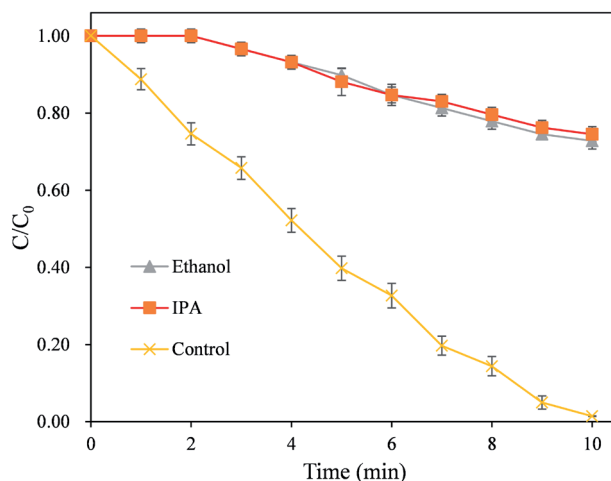


Fig. 6. The influence of ethanol and IPA on the degradation of CAP in the UV/PMS process. Conditions: initial concentration of CAP = 6  $\mu$ M, dosages of PMS = 0.4 mM, dosages of ethanol or IPA = 0.5 mM, temperature = 25°C, pH = 7.0, UV power = 14 W.

overall degradation efficiency of CAP plummeted, with comparable degrees of reduction observed. This led to the conclusion that  $\bullet$ OH was the dominant radical species in the oxidation process, aligning with previous findings from UV/PMS oxidation of haloacetonitriles [32].

## Model Analysis

Based on the BBD experimental setup, the coded factors and levels from Table 1 were input into Design-Expert 13 software, yielding 17 experimental schemes, which consisted of 5 center point replications and 12 factorial experiments. The experimental outcomes are presented in Table 3. By inputting the outcomes of these 17 experimental schemes into Design-Expert 13 software, a quadratic polynomial degradation model with degradation efficiency as the response variable and dosages of PMS, UV power, and retention time as independent variables were obtained, as shown in Equation (19).

$$Y = -1.20984 + 1.74311A + 0.12182B + 0.12584C + 0.014544AB - 8.06426 \times 10^3 AC + 3.51766 \times 10^4 BC - 1.20435A^2 - 5.25110 \times 10^3 B^2 - 4.72934 \times 10^3 C^2 \quad (19)$$

In the Equation, Y represents the degradation efficiency of CAP (non-dimensional), A stands for dosages of PMS (unit: mM), B represents UV power (unit: W), and C denotes retention time (unit: min).

Table 3. Experimental design matrix and the value of responses.

Run	Variables			Degradation efficiency of CAP	
	Dosages of PMS (mM)	UV power (W)	Retention time (min)	Actual	Predicted
1	0.5	3.5	4	16.45%	16.46%
2	0.2	8.75	14	63.38%	63.53%
3	0.5	8.75	9	84.78%	82.90%
4	0.5	14	14	98.62%	98.60%
5	0.5	3.5	14	54.28%	54.37%
6	0.5	8.75	9	84.78%	82.90%
7	0.2	3.5	9	21.13%	20.89%
8	0.5	8.75	9	80.27%	82.90%
9	0.5	8.75	9	79.93%	82.90%
10	0.8	3.5	9	51.78%	51.91%
11	0.8	14	9	98.64%	98.88%
12	0.2	14	9	58.82%	58.69%
13	0.8	8.75	4	59.52%	59.38%
14	0.5	8.75	9	84.78%	82.90%
15	0.5	14	4	57.09%	57.00%
16	0.8	8.75	14	96.94%	96.71%
17	0.2	8.75	4	21.13%	21.35%

Table 4. Analysis of variance for the quadratic model.

Source	Sum of Squares	df	Mean Square	F-value	P-value	Significance
Model	1.15	9	0.13	336.61	<0.0001	Significant
A-PMS	0.25	1	0.25	667.30	<0.0001	-
B-UV power	0.36	1	0.36	945.60	<0.0001	-
C-Time	0.32	1	0.32	831.87	<0.0001	-
AB	$2.099 \times 10^3$	1	$2.099 \times 10^3$	5.52	0.0511	-
AC	$5.853 \times 10^4$	1	$5.853 \times 10^4$	1.54	0.2545	-
BC	$3.411 \times 10^4$	1	$3.411 \times 10^4$	0.90	0.3750	-
A <sup>2</sup>	0.049	1	0.049	130.19	<0.0001	-
B <sup>2</sup>	0.088	1	0.088	232.12	<0.0001	-
C <sup>2</sup>	0.059	1	0.059	154.90	<0.0001	-
Residual	$2.660 \times 10^3$	7	$3.800 \times 10^4$	-	-	-
Lack of Fit	$3.118 \times 10^5$	3	$1.039 \times 10^5$	0.016	0.9968	Not significant
Pure Error	$2.629 \times 10^3$	4	$6.572 \times 10^4$	-	-	-
Cor Total	1.15	16	-	-	-	-

Statistical Analysis

The significance of the quadratic polynomial model was examined through Analysis of Variance (ANOVA). The ANOVA results were presented in Table 4, with the model fitting and error calculation by the Design-Expert 13 software. As established in the literature, the F-value and P-value are the most crucial indicators in model evaluation. A larger F-value and a smaller P-value

indicate a more significant model [41]. In the model, the P-value is primarily used to assess the significance of terms within the model. A model term is considered significant in the model if its P-value is less than 0.05; conversely, if the P-value is greater than 0.1, the model term is deemed insignificant.

For this quadratic polynomial model, the F-value of the model was 336.61, with a P-value <0.0001, indicating a high level of significance. The lack of fit F-value of

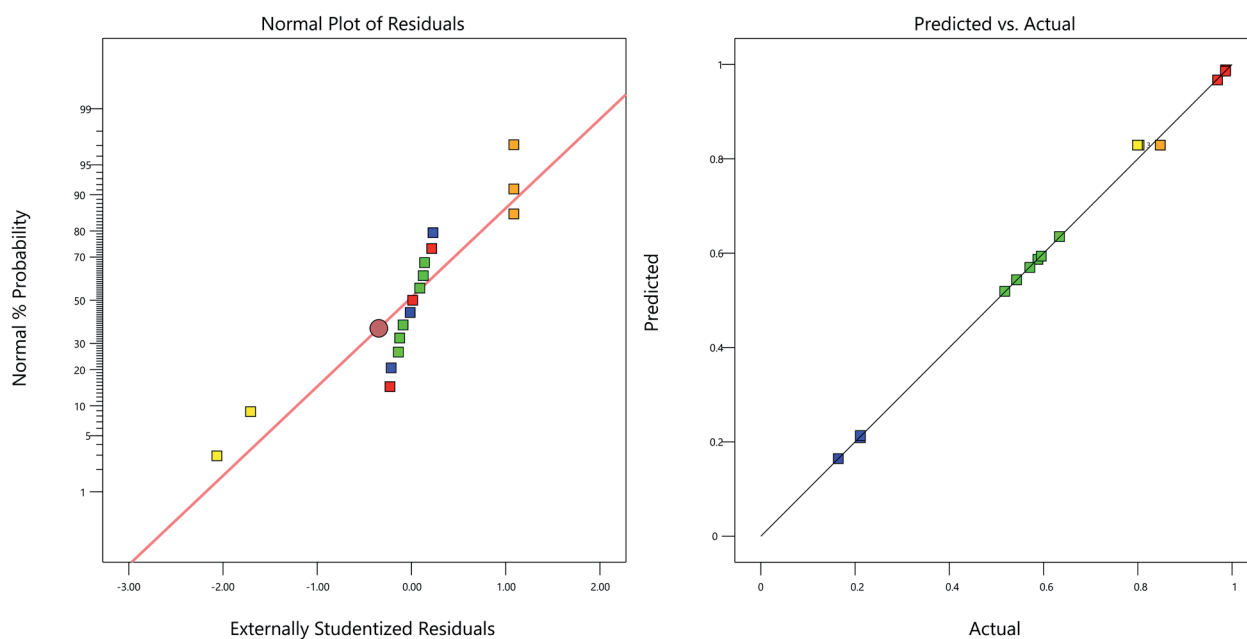


Fig. 7. Residual plots on CAP degradation by the VUV/PMS process. a) The normal plot of residual for 17 experimental values. b) Plot of predicted value versus experimental value.

0.016 implied that the lack of fit was not significant relative to the pure error. The “Pred R-Squared” of 0.9960 was in reasonable agreement with the “Adj R-Squared” of 0.9947. “Adeq Precision” measures the signal to noise ratio. A ratio greater than 4 is desirable. In the model, ratio of 55.127 indicated an adequate signal. This model could be used to navigate the design space. As illustrated in Fig. 7, the data points exhibited a linear distribution, indicating that the model residuals followed a normal distribution, thereby confirming the practical significance of the model. Furthermore, the actual values aligned closely with the predicted values, forming a nearly straight line with a strong linear correlation. This suggested an excellent fit between the model and the actual data, signifying that the model was capable of accurately predicting the degradation of CAP by the VUV/PMS process, achieving a satisfactory level of fitting performance.

### Factor Analysis

Contour and 3D response surface plots for the three factors were presented in Fig. 8. Spherical 3D response surfaces indicate negligible interaction among variables, whereas ellipsoidal or saddle-shaped plots signify more pronounced interactions among variables [23]. The 3D response surfaces revealed that the dosages of PMS, UV power, and retention time all significantly impact the degradation efficiency of CAP, with the degradation efficiency increasing as the independent variables increase. The influences of these three variables were relatively independent, with insignificant interactions among them. As evident from Table 3, the P-values for A, B, C, A<sup>2</sup>, B<sup>2</sup>, and C<sup>2</sup> were all less than 0.05, indicating their significance. Model terms with P-values greater than 0.1 were not significant, suggesting that AC and BC had negligible impacts on the model. The F-values for dosages of PMS dosage, UV power, and retention time were 667.30, 945.60, and 831.87, respectively, demonstrating that in the VUV/PMS degradation process for CAP, UV power had the greatest influence on the degradation rate, followed by retention time, and dosages of PMS had the least impact. Consequently, in practical applications, to enhance the degradation rate, priority should be given to increasing UV power, followed by extending retention time, and finally, an increase in dosages of PMS should be considered.

### Economic Optimization and Verification of the Mode

For the VUV/PMS process used in the degradation of CAP, the total operating cost comprises two main components: the electrical energy expenditure of the UV lamps and the cost of the oxidant. Regarding the electrical consumption of the process, following the guidelines of the International Union of Pure and Applied Chemistry (IUPAC), the economic efficiency of the photodegradation process is evaluated in terms

of the electrical energy per order (EE/O, kW·h/m<sup>3</sup>/order). EE/O is defined as the kilowatt-hour of electrical energy required to reduce the concentration of a pollutant by one order of magnitude in a 1 m<sup>3</sup> solution and can be calculated using Equation (20) [42, 43]. In this Equation, P represents the power of the UV lamp in kW, t is the irradiation time required to reduce the CAP concentration by one order of magnitude in minutes, and V denotes the volume of the reactant solution in m<sup>3</sup>.

$$EE/O = \frac{Pt}{60V} \quad (20)$$

Upon the aforementioned foundation, a new objective function Z was introduced, as depicted in Equation (21). Z represents the total operating cost of the process to reduce CAP in 1 m<sup>3</sup> of solution or wastewater by one order of magnitude, comprising both the electrical consumption cost and the oxidant cost. By substituting the unit prices of industrial electricity and the oxidant into Equation (21), Equation (22) was derived. A detailed calculation process is provided in Supplementary Material S2.

$$Z = EE/O \text{ cost} + \text{PMS cost} \quad (21)$$

Therefore, the problem was transformed into finding the minimum value of Eq. (22) under the constraints of Equations (23)-(26). In Equation (22), the unit of Z is USD/m<sup>3</sup>/order, where A represents the dosages of PMS in mM, B denotes the UV power in W, C is the reaction time required to achieve a 90% degradation efficiency in minutes, and Y refers to the quadratic polynomial in Equation (19), which signifies the degradation efficiency of CAP.

$$Z = 0.7816011A + 8.04917469 \times 10^{-4}BC \quad (22)$$

$$0.2 \leq A \leq 0.8 \quad (23)$$

$$3.5 \leq B \leq 14 \quad (24)$$

$$4 \leq C \leq 14 \quad (25)$$

$$90\% \leq Y \quad (26)$$

Equations (22)-(26) were input into MATLAB R2024a software, with the specific code provided in Supplementary Material S3. The VUV/PMS process achieved the lowest total operating cost for CAP degradation, amounting to 0.417 USD/m<sup>3</sup>/order, when the dosages of PMS were set at 0.3879 mM, the UV power at 11.4910 W, and the retention time at 12.3039 min. Under these optimal operating conditions, a model validation experiment was conducted, yielding a degradation efficiency of 96.89%, which was close to the model's predicted value of 90.00%. This demonstrated that the quadratic polynomial model effectively simulated the degradation of CAP by the VUV/PMS process, with reliable model outcomes and significant

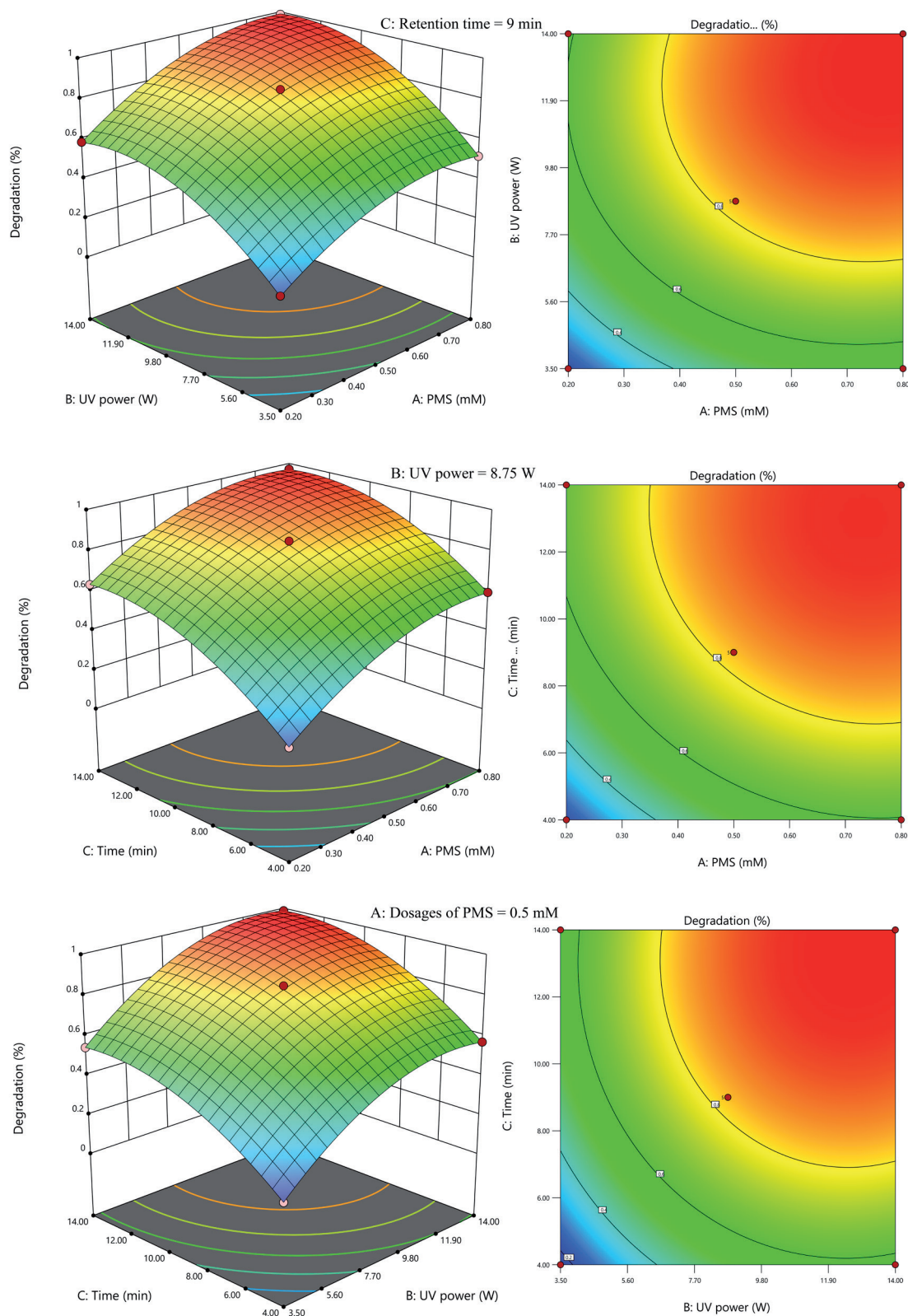


Fig. 8. Effects of dosages of PMS, UV power, and retention time on degradation efficiency of CAP.

practical application value. Furthermore, based on previous research findings on the degradation of CAP using UV-based advanced oxidation technology, it was evident that while effectively degrading CAP, this technology had also resulted in intermediate products of

CAP that exhibited significantly lower genetic toxicity compared to CAP itself [44]. In conclusion, the total operating cost as low as 0.417 USD/m<sup>3</sup>/order is highly valuable for process applications. The application of the VUV/PMS process in the actual degradation

treatment of CAP will drastically reduce both the electrical consumption and reagent costs associated with industrial CAP degradation, thus presenting a promising application prospect.

### Conclusions

The degradation efficiency of CAP by the VUV/PMS process was significantly greater than that of VUV and PMS individually. The degradation reaction followed pseudo-zero-order kinetics. Both acidic and alkaline conditions accelerated the reaction. Among the water matrix components, bicarbonate and nitrate ions exerted notable inhibitory effects, while chloride and sulfate ions had negligible impacts on the degradation efficiency. Hydroxyl radicals played a dominant role in the VUV/PMS oxidation process. RSM was employed to simulate and optimize the VUV/PMS oxidation process for CAP degradation. The quadratic polynomial model provided a satisfactory fit to the degradation process, with  $R^2$  and Adj- $R^2$  values of 0.9960 and 0.9947, respectively. Based on model optimization, when the dosages of PMS were set at 0.3879 mM, the UV power at 11.4910 W, and the retention time at 12.3039 min, the VUV/PMS process achieved the lowest total operating cost for CAP degradation, which was 0.417 USD/m<sup>3</sup>/order.

### Credit Authorship Contribution Statement

Xing Zhang: Writing - original draft. Jinghan Liu: Writing - review & editing, Project administration, Funding acquisition. Yizhi Liu: Writing - original draft, Validation. Changhua Lu: Writing - review & editing, Methodology, Supervision. Shuqing Li: Formal analysis. Zhen Zhou: Data curation.

### Acknowledgments

This work was supported by The Research and Development Fund of the Naval Logistics Academy (2024-17). Finally, Xing Zhang would like to thank his most beloved wife, Shuo Niu, for her support and love.

### Conflict of Interest

The authors declare no conflict of interest.

### References

1. WU L.J., YAN X.K., YANG L., SHEN S.T., LI Y.L., YANG S.D., HE L.Y., CHEN Y.L., YANG S.M., ZHANG Z.L. Simultaneous efficient degradation and dechlorination of chloramphenicol using UV/sulfite reduction: Mechanisms and product toxicity. *Chemical Engineering Journal*. **452**, 139161, **2023**.
2. FELISARDO R.J.A., BRILLAS E., FERREIRA L.F.R.F., CAVALCANTI E.B.C., GARCIA-SEGURA S. Degradation of the antibiotic ciprofloxacin in urine by electrochemical oxidation with a DSA anode. *Chemosphere*. **344**, 140407, **2023**.
3. ZHANG Y., YANG W.G., SU M.L., WANG B.W., YUAN R., LIANG W.B. A reagent-based label free electrochemiluminescence biosensor for ultrasensitive quantification of low-abundant chloramphenicol. *Microchemical Journal*. **198**, 110124, **2024**.
4. WANG Y.Q., DAI H.D., JIN M.T., WANG J.Y., SONG Z.H., LIU Y.J., CHAI W.Q., CHENG L., ZHAO N., CUI D.Z., ZHAO M. Light-driven biodegradation of chloramphenicol by photosensitized *Shewanella oneidensis* MR-1. *Bioresource Technology*. **413**, 131508, **2024**.
5. TRAN T.V., JALIL A.A., NGUYEN D.T.C., NGUYEN T.T.T., NGUYEN L.T.T., NGUYEN C.V., ALHASSAN M. Effect of pyrolysis temperature on characteristics and chloramphenicol adsorption performance of NH<sub>2</sub>-MIL-53(Al)-derived amine-functionalized porous carbons. *Chemosphere*. **355**, 141599, **2024**.
6. KIMOSOP S.J., GETENGA Z.M., ORATA F., OKELLO V.A., CHERUIYOT J.K. Residue levels and discharge loads of antibiotics in wastewater treatment plants (WWTPs), hospital lagoons, and rivers within Lake Victoria Basin, Kenya. *Environmental Monitoring and Assessment*. **188**, 532, **2016**.
7. TRAN N.H., CHEN H.J., REINHARD M., MAO F.J., GIN K.Y.H. Occurrence and removal of multiple classes of antibiotics and antimicrobial agents in biological wastewater treatment processes. *Water Research*. **104**, 461, **2016**.
8. MINH T.B., LEUNG H.W., LOI I.H., CHAN W.H., SO M.K., MAO J.Q., CHOI D., LAM J.C.W., ZHENG G., MARTIN M., LEE J.H.W., LAM P.K.S., RICHARDSON B.J. Antibiotics in the Hong Kong metropolitan area: Ubiquitous distribution and fate in Victoria Harbour. *Marine Pollution Bulletin*. **58**, 1052, **2009**.
9. TAHRANI L., LOCO J.V., MANSOUR H.B., REYNS T. Occurrence of antibiotics in pharmaceutical industrial wastewater, wastewater treatment plant and sea waters in Tunisia. *Journal of Water and Health*. **14**, 208, **2015**.
10. XU Y.L., LUO F., PAL A., GIN K.Y.H., REINHARD M. Occurrence of emerging organic contaminants in a tropical urban catchment in Singapore. *Chemosphere*. **83**, 963, **2011**.
11. PRAVEENA S.M., SHAIFUDDIN S.N.M., SUKIMAN S., NASIR F.A.M., HANAFI Z., KAMARUDIN N., ISMAIL T.H.T., ARIS A.Z. Pharmaceuticals residues in selected tropical surface water bodies from Selangor (Malaysia): Occurrence and potential risk assessments. *Science of The Total Environment*. **642**, 230, **2018**.
12. XU W.H., ZHANG G., ZOU S.C., LI X.D., LIU Y.C. Determination of selected antibiotics in the Victoria Harbour and the Pearl River, South China using high-performance liquid chromatography-electrospray ionization tandem mass spectrometry. *Environmental Pollution*. **145**, 672, **2007**.
13. JIANG L., HU X.L., YIN D.Q., ZHANG H.C., YU Z.Y. Occurrence, distribution and seasonal variation of antibiotics in the Huangpu River, Shanghai, China. *Chemosphere*. **82**, 822, **2011**.
14. WU L.J., YAN X.K., YANG L., SHEN S.T., LI Y.L., YANG S.D., HE L.Y., CHEN Y.L., YANG S.M., ZHANG Z.L. Simultaneous efficient degradation and dechlorination of chloramphenicol using UV/sulfite reduction:

- Mechanisms and product toxicity. *Chemical Engineering Journal*. **452**, 139161, **2023**.
15. BACANLI M., BAŞARAN N. Importance of antibiotic residues in animal food. *Food and Chemical Toxicology*. **125**, 462, **2019**.
  16. LIN J., ZHANG K.T., JIANG L.K., HOU J.F., YU X., FENG M.B., YE C.S. Removal of chloramphenicol antibiotics in natural and engineered water systems: Review of reaction mechanisms and product toxicity. *Science of The Total Environment*. **850**, 158059, **2022**.
  17. MAHDI M.H., MOHAMMED T.J., AL-NAJAR J.A. Advanced Oxidation Processes (AOPs) for treatment of antibiotics in wastewater: A review. *IOP Conference Series: Earth and Environmental Science*. **779**, 012109, **2021**.
  18. WANG Y.T., WANG J.Q., LONG Z.Q., SUN Z., LV L.Y., LIANG J.S., ZHANG G.M., WANG P.F., GAO W.F. MnCe-based catalysts for removal of organic pollutants in urban wastewater by advanced oxidation processes - A critical review. *Journal of Environmental Management*. **370**, 122773, **2024**.
  19. JAMIL T. Role of Advance Oxidation Processes (AOPs) in Textile Wastewater Treatment: A Critical Review. *Desalination and Water Treatment*. **318**, 100387, **2024**.
  20. GAO J., QIN T., WACŁAWEK S., DUAN X.D., HUANG Y., LIU H.Z., DIONYSIOS D.D. The application of advanced oxidation processes (AOPs) to treat unconventional water for fit-for-purpose reuse. *Current Opinion in Chemical Engineering*. **42**, 100974, **2023**.
  21. RIZZO L., LOFRANO G., GAGO C., BREDNEVA T., IANNECE P., PAZOS M., KRASNOGORSKAYA N., CAROTENUTO M. Antibiotic contaminated water treated by photo driven advanced oxidation processes: Ultraviolet/H<sub>2</sub>O<sub>2</sub> vs ultraviolet/peracetic acid. *Journal of Cleaner Production*. **205**, 67, **2018**.
  22. TAN C.Q., FU D.F., GAO N.Y., QIN Q.D., XU Y., XIANG H.M. Kinetic degradation of chloramphenicol in water by UV/persulfate system. *Journal of Photochemistry and Photobiology A: Chemistry*, **332**, 406, **2017**.
  23. VARANK G., CAN-GÜVEN E., GUVENC S.Y., GARAZADE N., TURK O.K., DEMIR A., CAKMAKCI M. Oxidative removal of oxytetracycline by UV-C/hydrogen peroxide and UV-C/peroxymonosulfate: Process optimization, kinetics, influence of co-existing ions, and quenching experiments. *Journal of Water Process Engineering*. **50**, 103327, **2022**.
  24. BELIKOV Y.A., SNYTNIKOVA O.A., SHEVEN D.G., FEDUNOV R.G., GRIVIN V.P., POZDNYAKOV I.P. Laser flash photolysis and quantum chemical studies of UV degradation of pharmaceutical drug chloramphenicol: Short-lived intermediates, quantum yields and mechanism of photolysis. *Chemosphere*. **351**, 141211, **2024**.
  25. XIE P.C., MA J., LIU W., ZOU J., YUE S.Y., LI X.C., WIESNER M.R., FANG J.Y. Removal of 2-MIB and geosmin using UV/persulfate: Contributions of hydroxyl and sulfate radicals. *Water Research*. **69**, 223, **2015**.
  26. MUSABEYGI T., GOUDARZI N., MIRZAEI M., ARAB-CHAMJANGALI M. Design of a ternary magnetic composite based on a covalent organic framework and Ag nanoparticles for simultaneous photodegradation of organic pollutants under LED light irradiation: Application of BBD-RSM modeling and resolution of spectral overlap of analytes. *Journal of Alloys and Compounds*. **964**, 171249, **2023**.
  27. SHAD A., CHEN J., QU R.J., DAR A.A., BIN-JUMAH M., ALLAM A.A., WANG Z.Y. Degradation of sulfadimethoxine in phosphate buffer solution by UV alone, UV/PMS and UV/H<sub>2</sub>O<sub>2</sub>: Kinetics, degradation products, and reaction pathways. *Chemical Engineering Journal*. **398**, 125357, **2020**.
  28. AO X.W., LIU W.J. Degradation of sulfamethoxazole by medium pressure UV and oxidants: Peroxymonosulfate, persulfate, and hydrogen peroxide. *Chemical Engineering Journal*. **313**, 629, **2017**.
  29. LING L., SUN J.L., FANG J.Y., SHANG C. Kinetics and mechanisms of degradation of chloroacetonitriles by the UV/H<sub>2</sub>O<sub>2</sub> process. *Water Research*. **99**, 209, **2016**.
  30. WANG Q., LU X.H., CAO Y., MA J., JIANG J., BAI X.F., HU T. Degradation of Bisphenol S by heat activated persulfate: Kinetics study, transformation pathways and influences of co-existing chemicals. *Chemical Engineering Journal*. **328**, 236, **2017**.
  31. ZHANG S.Y., ZOU J., CHEN L.X., ZHANG J.L., CUI H.Y., GONG C.M., HUANG Y.X., LIAO X.B., ZHOU Z.M. Chloride-enhanced ammonia removal in heat/peroxymonosulfate system: Production and contribution of chlorine. *Separation and Purification Technology*. **346**, 127441, **2024**.
  32. ZHANG X., YAO J.L., ZHAO Z.W., LIU J. Degradation of haloacetonitriles with UV/peroxymonosulfate process: Degradation pathway and the role of hydroxyl radicals. *Chemical Engineering Journal*. **364**, 1, **2019**.
  33. BUXTON G.V., GREENSTOCK C.L., HELMAN W.P., ROSS A.B. Critical Review of rate constants for reactions of hydrated electrons, hydrogen atoms and hydroxyl radicals in Aqueous Solution. *Journal of Physical and Chemical Reference Data*. **17**, 513, **1988**.
  34. KHAN J.A., HE X.X., KHAN H.M., SHAH N.S., DIONYSIOU D.D. Oxidative degradation of atrazine in aqueous solution by UV/H<sub>2</sub>O<sub>2</sub>/Fe<sup>2+</sup>, UV/S<sub>2</sub>O<sub>8</sub><sup>2-</sup>/Fe<sup>2+</sup> and UV/HSO<sub>5</sub><sup>-</sup>/Fe<sup>2+</sup> processes: A comparative study. *Chemical Engineering Journal*. **218**, 376, **2013**.
  35. WANG Z., DENG D.Y., YANG L.L. Degradation of dimethyl phthalate in solutions and soil slurries by persulfate at ambient temperature. *Journal of Hazardous Materials*. **271**, 202, **2014**.
  36. ZHANG X., YAO J.L., PENG W., XU W.S., LI Z.G., ZHOU C., FANG Z.D. Degradation of dichloroacetonitrile by a UV/peroxymonosulfate process: modeling and optimization based on response surface methodology (RSM). *RSC Advances*. **8**, 33681, **2018**.
  37. VERMA S., NAKAMURA S., SILLANPÄÄ M. Application of UV-C LED activated PMS for the degradation of anatoxin-a. *Chemical Engineering Journal*. **284**, 122, **2016**.
  38. IKEHATA K., EL-DIN M.G., SNYDER S.A. Ozonation and Advanced Oxidation Treatment of Emerging Organic Pollutants in Water and Wastewater. *Ozone: Science & Engineering*. **30**, 21, **2008**.
  39. SHAH N.S., HE X.X., KHAN H.M., KHAN J.A., O'SHEA K.E., BOCCELLI D.L., DIONYSIOU D.D. Efficient removal of endosulfan from aqueous solution by UV-C/peroxides: A comparative study. *Journal of Hazardous Materials*. **263**, 584, **2013**.
  40. WANG Y., ZHAO S., FAN W.C., TIAN Y., ZHAO X. The synthesis of novel Co–Al<sub>2</sub>O<sub>3</sub> nanofibrous membranes with efficient activation of peroxymonosulfate for bisphenol A degradation. *Environmental Science: Nano*. **5**, 1933, **2018**.
  41. MOHAMMED N.A., ALWARD A.I., SHAKHIR K.S., SULAIMAN F.A. Synthesis, characterization of FeNi<sub>3</sub>@SiO<sub>2</sub>/CuS for enhance solar photocatalytic degradation

- of atrazine herbicides: Application of RSM. Results in Surfaces and Interfaces. **16**, 100253, **2024**.
42. RAIKAR L.G., GANDHI J., GUPTA K.V.K., PRAKASH H. Degradation of Ampicillin with antibiotic activity removal using persulfate and submersible UVC LED: Kinetics, mechanism, electrical energy and cost analysis. Chemosphere. **349**, 140831, **2024**.
43. JENJAIWIT S., SIRIPATTANAKUL-RATPUKDI S., KHAN E., PRASOPSUK J., RATPUKDI T. Electro-

- peroxone process for triclocarban and triclosan removal and reclaimed water disinfection. Journal of Water Process Engineering. **67**, 106200, **2024**.
44. JIN Q.Q., WANG H.B., HU C., CHEN Z.S., WANG X.K. Effects of NOM on the degradation of chloramphenicol by UV/H<sub>2</sub>O<sub>2</sub> and the characteristics of degradation products. Separation and Purification Technology. **191**, 108, **2018**.

## Supplementary Material

S1

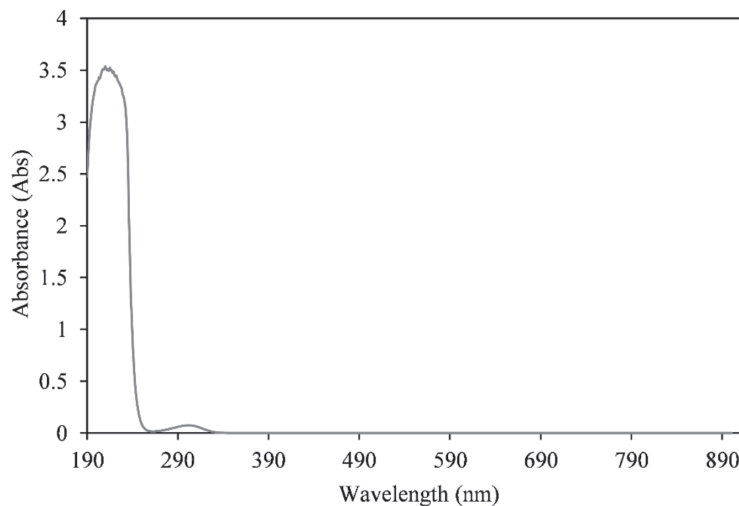


Fig. S1. The full spectrum scanning of 10 mM sodium nitrate.

S2

### Detailed Procedure of EE/O Computation

$$\begin{aligned} \text{EE/O} &= \text{Pt}/(60\text{V}) = \text{UV power} \times \text{T}/(60 \times 0.002) \\ &= 8.33333 \times 10^{-3} \times \text{UV power} \times \text{T} \end{aligned}$$

In the Equation, EE/O represents the kilowatt-hours (kWh) of electrical energy required to reduce the pollutant concentration by one order of magnitude in a 1 m<sup>3</sup> solution, with units of kWh/m<sup>3</sup>/order. UV power denotes the power of the ultraviolet lamp, measured in watts (W). T represents the time taken for a 90% degradation efficiency, in minutes.

As of June 2024, the industrial electricity price in China, as provided by State Grid Hebei, is 0.70221 CNY per kilowatt-hour.

$$\begin{aligned} \text{EE/O cost} &= 8.33333 \times 10^{-3} \times \text{UV power} \times \text{T} \\ &\times 0.70221 = 5.85175 \times 10^{-3} \times \text{UV power} \times \text{T} \end{aligned}$$

In the Equation, EE/O cost represents the electrical cost required to reduce the concentration of pollutants by one order of magnitude, expressed in units of Chinese yuan per cubic meter per order (CNY/m<sup>3</sup>/order).

### Chemical Cost Calculation:

The unit price of Oxone was 16 CNY per kilogram, with an active material content of 42.8%, referring to the weight percentage of KHSO<sub>5</sub> in the composite salt.

$$\begin{aligned} 1 \text{ kg Oxone} &= 0.428 \text{ kg KHSO}_5 = 428/152 \text{ mol} \\ \text{KHSO}_5 &= 2.81579 \text{ mol KHSO}_5 \end{aligned}$$

As a result, the unit price of  $\text{KHSO}_5$  was calculated as 16/2.81579, equaling 5.68224 CNY per mole.

$$\text{PMS cost} = \text{dosages of PMS} \times 10^{-3} \times 2 \\ \times 5.68224/0.002 = 5.68224 \times \text{dosages of PMS}$$

In the equation, PMS cost represents the expenditure of oxidant required to reduce the concentration of pollutants by one order of magnitude, expressed in units of CNY/m<sup>3</sup>/order. The dosages of PMS are measured in mM.

### Total Operating Cost

Objective function

$$Z = \text{EE/O cost} + \text{PMS cost} = (5.85175 \times 10^{-3} \times \text{UV} \\ \text{power} \times T + 5.68224 \times \text{dosages of PMS})/7.27 \\ = 0.7816011 \times \text{dosages of PMS} + 8.04917469 \times 10^{-4} \\ \times \text{UV power} \times T$$

In the Equation, Z represents the total operating cost of the process to reduce CAP in 1 m<sup>3</sup> of solution or wastewater by one order of magnitude, expressed in units of USD/m<sup>3</sup>/order. UV power represents the power of the ultraviolet lamp, measured in W. T represents the time taken to achieve a 90% degradation rate, measured in min. Dosages of PMS denotes the concentration of PMS, measured in mM.

To find the minimum value of the objective function Z.

$$Z = 0.7816011A + 8.04917469 \times 10^{-4}BC$$

Constraint conditions:

- (1)  $0.2 \leq A \leq 0.8$
- (2)  $3.5 \leq B \leq 14$
- (3)  $4 \leq C \leq 14$
- (4)  $90\% \leq -1.26358 + 1.83099A + 0.12684B + 0.13153C \\ + 0.014544AB - 0.00806426AC + 0.000351766BC \\ - 1.29223A^2 - 0.00553804B^2 - 0.0050457C^2$

### S3

% Define the objective function  
function f = objectiveFunction(x)

$$f = 0.7816011 * x(1) + 8.04917469e-4 * x(2) \\ * x(3);$$

end

% Defined nonlinear constraint

function [c, ceq] = nonlinearConstraints(x)  
c = [];

$$\text{ceq} = -1.20984 + 1.74311*x(1) + 0.12182*x(2) \\ + 0.12584*x(3) + 0.014544*x(1)*x(2) \\ - 0.00806426*x(1)*x(3) + 0.000351766*x(2)*x(3) \\ - 1.20435*x(1)^2 - 0.0052511*x(2)^2 \\ - 0.00472934*x(3)^2 - 0.9;$$

end

% Set the initial guess

x0 = [0.5, 8, 9];

% Set constraints

lb = [0.2, 3.5, 4];

ub = [0.8, 14, 14];

% Call the fmincon function for optimization

options = optimoptions('fmincon', 'Display', 'iter');

[x, fval] = fmincon(@objectiveFunction, x0, [], [], [], [], lb, ub, @nonlinearConstraints, options);

% Output result

disp(' The optimal solution:');

disp(x);

disp(' minimum value:');

disp(fval);